Stability of modulated finite-gap cylindrical Couette flow: linear theory

By S. CARMI AND J. I. TUSTANIWSKYJ

Department of Mechanical Engineering,
Wayne State University, Detroit, Michigan 48202

The linear stability of an extensively modulated cylindrical Couette flow is investigated in the finite-gap range. A closed form analytic solution is obtained for the basic unsteady flow after modulation is introduced through the boundary conditions. The general linear perturbation equations for three-dimensional disturbances are then derived and subsequently solved using the Galerkin method with the stability analysed by the Floquet theory. Modulation is found to destabilize the flow in most cases and results compare very favourably with the ones obtained experimentally. Stabilization is possible only for some cases of outer cylinder modulation.

1. Introduction

The stability of time-dependent flows has recently attracted the attention of a number of investigators. The linear and nonlinear theories were employed with various degrees of success. A rather extensive review was recently published by Davis (1976). In the current paper we will employ the linear theory to study the stability of time-dependent fluid flow between two concentric cylinders.

A common geophysical fluid dynamic laboratory experiment involves fluid flow between two rotating concentric cylinders (often referred to as circular Couette or Taylor flow). The experimental as well as the theoretical work on this type of flow has been used to model jet streams, fronts and atmospheric waves with imbedded cyclones (see review by Hide 1969). Recently Clever, Busse & Kelly (1977) applied the Taylor instability problem in their study of atmospheric convective rolls in the planetary boundary layer, which give rise to cloud-street formations. In industrial applications the study of circular Couette flow is important in lubrication mechanics and viscosity measurements.

Many of the flows mentioned above as well as most flows occurring in nature are unsteady. Of all time-dependent flows and processes observed either in nature or in the laboratory, periodic or semi-periodic systems constitute the largest and perhaps the most important subset. Some fascinating examples occur in biochemical systems. Spatial and temporal oscillations of concentrations accompanied by dramatic colour changes have been observed in the so called 'Belousov–Zhabotinskii' reaction. This chemical reaction is essentially the oxidation of malonic acid by bromate in the presence of a cerium catalyst. Its importance is that it mirrors biological oscillators, which are believed to perform intercellular communication in living tissues (see review by Othmer 1976). Another important example from the biological sciences is found in the study of the stability of the flow in the aorta. The two major phenomena in this

connection are discussed by Seminara & Hall (1976), one being the oscillatory pressure gradient driving the blood flow, the second being the curvature in the pipe which increases the prospect of centrifugal instability. In the study of global circulation patterns, periodic growth and decay of the amplitude of baroclinic waves has been observed (see Pedlosky 1972). An important industrial application of periodic flow is the high speed non-impact printer, which depends on a sinusoidally excited jet stream to form ink droplets. There are numerous other examples but for the sake of brevity, we will confine ourselves to the ones mentioned above.

In this work we studied the flow between two concentric cylinders whose walls located at $r = R_1$ and $r = R_2$ are rotating with constant angular velocities Ω_1 and Ω_2, respectively, and with modulation performed on both of them. In addition, we also examined modulation performed on stationary cylinders (zero-mean case). No narrow-gap limit is assumed throughout this work.

A closed-form analytic solution is derived for the basic unsteady flow in terms of modified Bessel functions after the governing equations in the given domain are solved satisfying the modulated boundary conditions.

Next, the linear perturbation equations governing disturbances in modulated flow are derived for the general three-dimensional case which includes both axial and azimuthal disturbances. After introducing normal modes the two dependent variables u and v are expanded into Galerkin series with time-dependent coefficients. The remaining spatial dependence is then absorbed into coefficients via integration over the x domain, while the temporal dependence is cast into a first-order system of ordinary differential equations in time. The stability of this system is then analysed by employing the Floquet theory. Our numerical scheme was adopted to work for different values of the modulation amplitudes and frequencies. Stability limits are obtained as a converging sequence for an increasing order of Galerkin expansions. For the zero-mean flow problem (modulation in the stationary case) we found that higher-order Galerkin expansions are needed at higher frequencies. In the narrow gap limit for zero-mean flows, our results show some qualitative agreement with those of Riley & Laurence (1976) but no jump discontinuities were found in the critical wavenumber and frequency plane (see the appendix). For non-zero-mean flows (again in the narrow-gap limit) our findings coincide with those of Hall (1975) but agreement with Riley & Laurence is seen only for small amplitudes of modulation.

A close correlation between Thompson's (1968) experimental observations and the results of the present investigation constitutes an important step in enhancing their significance in atmospheric fluid dynamic situations. A detailed derivation and discussion of the present results can be found in Tustaniwskyj (1979).

2. Modulated basic flow and linear perturbation formulation

The equations governing the basic flow are

$$\frac{\partial \mathbf{u}}{\partial t} + (\mathbf{u} . \nabla) \mathbf{u} = \frac{-1}{\rho} \nabla p + \nu \nabla^2 \mathbf{u}, \tag{1}$$

and
$$\nabla . \mathbf{u} = 0. \tag{2}$$

Here we utilize cylindrical polar co-ordinates (r, θ, z), where the z axis is the common axis of the cylinders located at $r = R_1$ and $r = R_2$, with $R_1 < R_2$.

The basic flow is azimuthal, and is generated by the motion of one or both the cylinders. The velocity vector of this basic flow thus has the form

$$\mathbf{u} = (0, V(r,t), 0). \tag{3}$$

We restrict ourselves to basic modulated flows which are time periodic with period $2\pi/\omega$. In this case $V(r,t)$ satisfies

$$\frac{\partial V}{\partial t} = \nu\left[\frac{\partial^2 V}{\partial r^2} + \frac{1}{r}\frac{\partial V}{\partial r} - \frac{V}{r^2}\right], \tag{4}$$

with boundary conditions

$$V(R_1, t) = R_1(\Omega_1 + \epsilon_1 \cos \omega t), \tag{5}$$

$$V(R_2, t) = R_2(\Omega_2 + \epsilon_2 \cos \omega t). \tag{6}$$

It is convenient to decompose the velocity field $V(r,t)$ into steady and periodic parts

$$V(r,t) = V_s(r) + V_p(r,t), \tag{7}$$

obtained by solving (4)–(6). The steady part is

$$V_s = \bar{A}r + \bar{B}/r, \tag{8}$$

where

$$\bar{A} = \frac{\Omega_2 R_2^2 - \Omega_1 R_1^2}{R_2^2 - R_1^2}, \quad \bar{B} = \frac{(\Omega_1 - \Omega_2)R_2^2 R_1^2}{R_2^2 - R_1^2}.$$

For the time periodic part we get

$$V_p = \mathrm{Re}\left[\left\{\epsilon_1\left(S_1 I_1\left(\left(\frac{i\omega}{\nu}\right)^{\frac{1}{2}}r\right) - T_1 K_1\left(\left(\frac{i\omega}{\nu}\right)^{\frac{1}{2}}r\right)\right)\right.\right.$$
$$\left.\left. + \epsilon_2\left(T_2 K_1\left(\left(\frac{i\omega}{\nu}\right)^{\frac{1}{2}}r\right) - S_2 I_1\left(\left(\frac{i\omega}{\nu}\right)^{\frac{1}{2}}r\right)\right)\right\}e^{i\omega t}\right], \tag{9}$$

where I_1 and K_1 are modified Bessel functions and

$$S_1 = R_1 K_1\left(\left(\frac{i\omega}{\nu}\right)^{\frac{1}{2}}R_2\right)\Big/\Delta, \quad S_2 = R_2 K_1\left(\left(\frac{i\omega}{\nu}\right)^{\frac{1}{2}}R_1\right)\Big/\Delta,$$

$$T_1 = R_1 I_1\left(\left(\frac{i\omega}{\nu}\right)^{\frac{1}{2}}R_2\right)\Big/\Delta, \quad T_2 = R_2 I_1\left(\left(\frac{i\omega}{\nu}\right)^{\frac{1}{2}}R_1\right)\Big/\Delta,$$

with

$$\Delta = I_1\left(\left(\frac{i\omega}{\nu}\right)^{\frac{1}{2}}R_1\right)K_1\left(\left(\frac{i\omega}{\nu}\right)^{\frac{1}{2}}R_2\right) - I_1\left(\left(\frac{i\omega}{\nu}\right)^{\frac{1}{2}}R_2\right)K_1\left(\left(\frac{i\omega}{\nu}\right)^{\frac{1}{2}}R_1\right).$$

Associated with the basic velocity field (7) is a pressure field $P(r,t)$ which is given by

$$\frac{\partial P}{\partial r} = \rho\frac{V^2}{r}. \tag{10}$$

The equations governing infinitesimal disturbances of the modulated flow (7) are obtained by substituting

$$u = u(r, \theta, z, t), \quad v = V(r,t) + v(r, \theta, z, t),$$
$$w = w(r, \theta, z, t), \quad p = P(r,t) + p(r, \theta, z, t),$$

into (1) and (2) and neglecting second- and higher-order terms. The disturbances u, v, w and p can be Fourier analysed with respect to θ and z:

$$
\begin{aligned}
u(r,\theta,z,t) &= \hat{u}(r,t)\cos kz\cos n\theta + \acute{u}(r,t)\cos kz\sin n\theta,\\
v(r,\theta,z,t) &= \hat{v}(r,t)\cos kz\cos n\theta + \acute{v}(r,t)\cos kz\sin n\theta,\\
w(r,\theta,z,t) &= \hat{w}(r,t)\sin kz\cos n\theta + \acute{w}(r,t)\sin kz\sin n\theta,\\
p(r,\theta,z,t) &= \hat{p}(r,t)\cos kz\cos n\theta + \acute{p}(r,t)\cos kz\sin n\theta.
\end{aligned}
\tag{11}
$$

Substituting (11) into the linear perturbation equations and after elimination of $\hat{p}$, $\acute{p}$, $\hat{w}$, $\acute{w}$ from the resulting equations and the introduction of non-dimensional variables

$$
x = (r-R_1)/d - \tfrac{1}{2} \quad \text{and} \quad \tau = \omega t,
$$

we obtain the governing equations for $\hat{u}$, $\acute{u}$, $\hat{v}$, $\acute{v}$,

$$
\begin{aligned}
&\sigma\frac{\partial}{\partial\tau}\left(L\hat{u}+nD\left(\frac{\acute{v}}{\beta}\right)\right)-\frac{d}{\nu}\frac{Vna^2}{\beta}\acute{u}+\frac{d}{\nu}\frac{2a^2V\hat{v}}{\beta}+\frac{nd}{\nu}\frac{DV}{\beta}\left(\frac{\acute{u}}{\beta}+Du\right)\\
&\quad+\frac{nd}{\nu}\frac{V}{\beta}\left(D^2\acute{u}-\frac{2\acute{u}}{\beta^2}\right)-\frac{n^2d}{\nu}\frac{DV\hat{v}}{\beta^2}-\frac{n^2dV}{\nu\beta^2}\left(D\hat{v}-\frac{2\hat{v}}{\beta}\right)\\
&\quad= L_nL\hat{u}-\frac{L\hat{u}}{\beta^2}+\frac{2n^2}{\beta^3}\left(D\hat{u}+\frac{\hat{u}}{\beta}\right)+\frac{2na^2}{\beta^2}\acute{v}+nDL_n\left(\frac{\acute{v}}{\beta}\right),\\[6pt]
&\sigma\frac{\partial}{\partial\tau}\left(L\acute{u}-nD\left(\frac{\hat{v}}{\beta}\right)\right)+\frac{d}{\nu}\frac{Vna^2}{\beta}\hat{u}+\frac{d}{\nu}\frac{2a^2V\acute{v}}{\beta}-\frac{nd}{\nu}\frac{DV}{\beta}\left(\frac{\hat{u}}{\beta}+D\hat{u}\right)\\
&\quad-\frac{nd}{\nu}\frac{V}{\beta}\left(D^2\hat{u}-\frac{2\hat{u}}{\beta^2}\right)-\frac{n^2d}{\nu}\frac{DVv}{\beta^2}-\frac{n^2dV}{\nu\beta^2}\left(Dv-\frac{2v}{\beta}\right)\\
&\quad= L_nL\acute{u}-\frac{L\acute{u}}{\beta^2}+\frac{2n^2}{\beta^3}\left(D\acute{u}+\frac{\acute{u}}{\beta}\right)-\frac{2na^2}{\beta^2}\hat{v}-nDL_n\left(\frac{\hat{v}}{\beta}\right),\\[6pt]
&\sigma\frac{\partial}{\partial\tau}\left(a^2\hat{v}-\frac{n}{\beta}\left(\frac{\acute{u}}{\beta}+D\acute{u}\right)+\frac{n^2}{\beta^2}\hat{v}\right)+\frac{d}{\nu}\frac{n^2V}{\beta^2}\left(\frac{\hat{u}}{\beta}+D\hat{u}\right)+\frac{d}{\nu}\frac{n^3}{\beta^3}V\acute{v}\\
&\quad+\frac{d}{\nu}a^2DV\hat{u}+\frac{d}{\nu}\frac{a^2n}{\beta}V\acute{v}+\frac{d}{\nu}\frac{a^2}{\beta}V\hat{u}\\
&\quad= a^2L\hat{v}-\frac{a^2n^2}{\beta^2}\hat{v}+\frac{2na^2}{\beta^2}\acute{u}-\frac{n}{\beta}L_n\left(\frac{\acute{u}}{\beta}+D\acute{u}\right)+\frac{n^2}{\beta}L_n\left(\frac{\hat{v}}{\beta}\right),\\[6pt]
&\sigma\frac{\partial}{\partial\tau}\left(a^2\acute{v}+\frac{n}{\beta}\left(\frac{\hat{u}}{\beta}+D\hat{u}\right)+\frac{n^2}{\beta^2}\acute{v}\right)+\frac{d}{\nu}\frac{n^2V}{\beta^2}\left(\frac{\acute{u}}{\beta}+D\acute{u}\right)-\frac{d}{\nu}\frac{n^3}{\beta^3}V\hat{v}\\
&\quad+\frac{d}{\nu}a^2DV\acute{u}-\frac{d}{\nu}\frac{a^2n}{\beta}V\hat{v}+\frac{d}{\nu}\frac{a^2}{\beta^2}V\acute{u}\\
&\quad= a^2L\acute{v}-\frac{a^2n^2}{\beta^2}\acute{v}-\frac{2na^2}{\beta^2}\hat{u}+\frac{n}{\beta}L_n\left(\frac{\hat{u}}{\beta}+D\hat{u}\right)+\frac{n^2}{\beta}L_n\left(\frac{\acute{v}}{\beta}\right),
\end{aligned}
\tag{12}
$$

where

$$
d = R_2-R_1, \quad \sigma = \frac{\omega d^2}{\nu}, \quad a = kd,
$$

$$
X_1 = \frac{R_1}{d}, \quad D = \frac{\partial}{\partial x}, \quad \beta = x+\tfrac{1}{2}+X_1,
$$

$$
L = D^2+\frac{D}{\beta}-\frac{1}{\beta^2}-a^2, \quad L_n = D^2+\frac{D}{\beta}-\frac{n^2}{\beta^2}-a^2.
$$

These equations are subject to the boundary conditions

$$\hat{u} = \acute{u} = D\hat{u} = D\acute{u} = \hat{v} = \acute{v} = 0 \quad \text{at} \quad x = \pm \tfrac{1}{2}. \tag{13}$$

3. Stability analysis and numerical procedure

We first seek a solution to the general linear perturbation equations (12), (13) where three-dimensional disturbances ($n \neq 0$, $k \neq 0$) are allowed. The perturbation variables $\hat{u}, \acute{u}, \hat{v}, \acute{v}$ are expanded into a Galerkin series

$$\hat{v} = \sum_{m=1}^{M} A_m(\tau) v_m(x), \quad \acute{v} = \sum_{m=1}^{M} B_m(\tau) v_m(x), \\ \hat{u} = \sum_{m=1}^{M} C_m(\tau) u_m(x), \quad \acute{u} = \sum_{m=1}^{M} E_m(\tau) u_m(x). \tag{14}$$

The functions

$$v_m(x) = \sqrt{2} \sin m\pi(\tfrac{1}{2} - x), \tag{15}$$

and

$$u_m(x) = \frac{\sinh(\xi_m x + \tfrac{1}{2}im\pi)}{\sinh \tfrac{1}{2}(\xi_m + im\pi)} - \frac{\sin(\xi_m x + \tfrac{1}{2}m\pi)}{\sin \tfrac{1}{2}(\xi_m + m\pi)}, \tag{16}$$

where ξ_m are consecutive positive roots of

$$\tanh \tfrac{1}{2}\xi_m = (-1)^m \tan \tfrac{1}{2}\xi_m,$$

constitute complete orthonormal sets and are solutions of

$$D^2 v_m + m^2\pi^2 v_m = 0, \quad v_m = 0 \quad \text{at} \quad x \pm \tfrac{1}{2},$$

and

$$D^4 u_m = \xi_m^4 u_m, \quad u_m = Du_m = 0 \quad \text{at} \quad x = \pm \tfrac{1}{2}, \quad \text{respectively.}$$

Substituting (14) into the linear perturbation equations yields

$$\sum_{m=1}^{M} \dot{C}_m L u_m + n \sum_{m=1}^{M} \dot{B}_m D\left[\frac{v_m}{\beta}\right] \\ = \frac{d}{\sigma\nu} \sum_{m=1}^{M} E_m \Phi_m + \frac{d}{\sigma\nu} \sum_{m=1}^{M} A_m \Psi_m + \frac{1}{\sigma} \sum_{m=1}^{M} \Gamma_m C_m + \frac{1}{\sigma} \sum_{m=1}^{M} \Theta_m B_m, \tag{17}$$

$$\sum_{m=1}^{M} \dot{E}_m L u_m - n \sum_{m=1}^{M} \dot{A}_m D\left[\frac{v_m}{\beta}\right] \\ = -\frac{d}{\sigma\nu} \sum_{m=1}^{M} C_m \Phi_m + \frac{d}{\sigma\nu} \sum_{m=1}^{M} B_m \Psi_m + \frac{1}{\sigma} \sum_{m=1}^{M} \Gamma_m E_m - \frac{1}{\sigma} \sum_{m=1}^{M} \Theta_m A_m, \tag{18}$$

$$\sum_{m=1}^{M} \dot{A}_m \left[a^2 + \frac{n^2}{\beta^2}\right] v_m - \sum_{m=1}^{M} \frac{n}{\beta}\left[\frac{u_m}{\beta} + Du_m\right] \dot{E}_m \\ = \frac{d}{\sigma\nu} \sum_{m=1}^{M} C_m \Upsilon_m - \frac{d}{\sigma\nu} \sum_{m=1}^{M} B_m \Pi_m + \frac{1}{\sigma} A_m \Xi_m - \frac{1}{\sigma} \sum_{m=1}^{M} \chi_m E_m, \tag{19}$$

$$\sum_{m=1}^{M} \dot{B}_m \left[a^2 + \frac{n^2}{\beta^2}\right] v_m + \sum_{m=1}^{M} \frac{n}{\beta}\left[\frac{u_m}{\beta} + Du_m\right] \dot{C}_m \\ = \frac{d}{\sigma\nu} \sum_{m=1}^{M} E_m \Upsilon_m + \frac{d}{\sigma\nu} \sum_{m=1}^{M} A_m \Pi_m + \frac{1}{\sigma} \sum_{m=1}^{M} B_m \Xi_m + \frac{1}{\sigma} \chi_m C_m, \tag{20}$$

where

$$\Phi_m = \frac{n}{\beta}\left[Va^2 u_m - DV\left[\frac{u_m}{\beta} + Du_m\right] - V\left[D^2 u_m - \frac{2u_m}{\beta^2}\right]\right],$$

$$\Psi_m = -\frac{2a^2 V v_m}{\beta} + \frac{n^2 DV v_m}{\beta^2} + \frac{n^2 V}{\beta^2}\left[Dv_m - \frac{2v_m}{\beta}\right],$$

$$\Gamma_m = L^2 u_m - \frac{n^2}{\beta^2}Lu_m + \frac{2n^2}{\beta^3}\left[Du_m + \frac{u_m}{\beta}\right],$$

$$\Theta_m = n\left[\frac{2a^2}{\beta^2}v_m + DL_n\left[\frac{v_m}{\beta}\right]\right],$$

$$\Upsilon_m = -\frac{Vn^2}{\beta^2}\left[\frac{u_m}{\beta} + Du_m\right] - a^2 DV u_m - \frac{a^2 V u_m}{\beta},$$

$$\Pi_m = \frac{nV}{\beta}\left[\frac{n^2}{\beta^2} + a^2\right]v_m,$$

$$\Xi_m = a^2 Lv_m + \frac{n^2}{\beta}\left[L_n\left[\frac{v_m}{\beta}\right] - \frac{a^2 v_m}{\beta}\right],$$

$$\chi_m = -\frac{n}{\beta}\left[\frac{2a^2 u_m}{\beta} - L_n\left[\frac{u_m}{\beta} + Du_m\right]\right].$$

Next we multiply (17), (18), (19), (20) by u_l, iu_l, v_l and iv_l, respectively, and integrate over the range $(-\frac{1}{2}, \frac{1}{2})$ to get $2M$ sets of complex equations which can be written in the form

$$C_{ij}\dot{q}_j = D'_{ij}(\tau)q_j, \quad i, j = 1, 2, 3, \ldots, 2M, \tag{21}$$

where

$$q_1 = A_1 + iB_1, \quad q_{M+1} = C_1 + iE_1,$$

$$q_2 = A_2 + iB_2, \quad q_{M+2} = C_2 + iE_2, \quad \text{etc.};$$

$$\mathbf{C} = \left[\begin{array}{c|c} \mathbf{Y} & i\mathbf{S} \\ \hline -i\mathbf{G} & \mathbf{F} \end{array}\right],$$

$$\mathbf{D}' = \left[\begin{array}{c|c} \mathbf{R}+i\mathbf{X} & \mathbf{T}+i\mathbf{P} \\ \hline \mathbf{K}-i\mathbf{Q} & \mathbf{Z}-i\mathbf{H} \end{array}\right],$$

with

$$Y_{lm} = \left\langle v_l, \left[a^2 + \frac{n^2}{\beta^2}\right]v_m\right\rangle, \quad S_{lm} = \left\langle v_l, \frac{n}{\beta}\left[\frac{u_m}{\beta} + Du_m\right]\right\rangle,$$

$$F_{lm} = \langle u_l, Lu_m\rangle, \quad G_{lm} = n\left\langle u_l, D\left[\frac{v_m}{\beta}\right]\right\rangle,$$

$$R_{lm} = \frac{1}{\sigma}\langle v_l, \Xi_m\rangle, \quad X_{lm} = \frac{d}{\sigma\nu}\langle v_l, \Pi_m\rangle,$$

$$T_{lm} = \frac{d}{\sigma\nu}\langle v_l, \Upsilon_m\rangle, \quad P_{lm} = \frac{1}{\sigma}\langle v_l, \chi_m\rangle,$$

$$K_{lm} = \frac{d}{\sigma\nu}\langle u_l, \Psi_m\rangle, \quad Q_{lm} = \frac{1}{\sigma}\langle u_l, \Theta_m\rangle,$$

$$Z_{lm} = \frac{1}{\sigma}\langle u_l, \Gamma_m\rangle, \quad H_{lm} = \frac{d}{\sigma\nu}\langle u_l, \Phi_m\rangle,$$

and

$$\langle \alpha, \eta\rangle = \int_{-\frac{1}{2}}^{\frac{1}{2}} \alpha\eta\, dx.$$

Multiplying (21) by the inverse of **C**, the equations are uncoupled yielding

$$\dot{q}_1 = D_{ij}(\tau)\, q_j, \quad i,j = 1, 2, 3, \ldots, 2M, \tag{22}$$

where

$$\mathbf{D} = \mathbf{C}^{-1}\mathbf{D}'.$$

Our problem is now reduced to analysing the stability of the system (22). This will be accomplished using the classical Floquet theory and numerical methods to be described next. Let

$$q_i^{(n)}(\tau) = \mathrm{col}\,[q_1^{(n)}(\tau), \ldots, q_{2M}^{(n)}(\tau)], \tag{23}$$

be a solution of (22) which satisfied the initial conditions

$$q_i^{(n)} = \delta_{in}, \tag{24}$$

with $n = 1, 2, \ldots, 2M$. The $2M$ linearly independent $q_i^{(n)}(2\pi)$, obtained by integrating (22), are arranged in a $2M \times 2M$ matrix **P**. The eigenvalues $\lambda_1, \ldots, \lambda_{2M}$ of the matrix **P** are the characteristic multipliers of (22) with the characteristic exponents μ_r defined by

$$\lambda_r = e^{2\pi\mu_r}.$$

Ordering the characteristic exponents

$$\mathrm{Re}\,(\mu_1) \geqslant \mathrm{Re}\,(\mu_2) \geqslant \ldots \geqslant \mathrm{Re}\,(\mu_{2M})$$

we find the system to be stable if $\mathrm{Re}\,(\mu_1) < 0$, while $\mathrm{Re}\,(\mu_1) = 0$ defines a stability boundary and corresponds to one periodic solution.

Our numerical integration technique consists of a forward integration scheme in the complex domain coupled with a root finder method for determining the stability limits as eigenvalues.

All numerical work was performed with double precision on the Wayne State University Computing Center's Amdahl 470 V-6 computer system. Complex Bessel functions were evaluated using small and large argument polynomial expansions (see Abramowitz & Stegun 1972). An adaptive Romberg extrapolation procedure was used to obtain the coefficients of the $D_{ij}(\tau)$ matrix. The relative error of these coefficients was estimated to be less than 10^{-4}. Forward integration in time had to be performed using an incremental modal analysis technique, since the system (22) had proved to be stiff. In this procedure we assume that matrix D_{ij} remains constant over the time interval τ to $\tau + \Delta\tau$. Here we evaluate the eigenvalues and eigenvectors of matrix D_{ij} at time τ, transform co-ordinates $q_i(\tau)$ to modal co-ordinates $q_i^*(\tau)$, integrate in the modal domain to obtain $q_i^*(\tau + \Delta\tau)$, and then transform it back to $q_i(\tau + \Delta\tau)$. We found that with this integration procedure our stability limit would converge to four significant digits when a time step of $2\pi/30$ was chosen. For zero-mean flows, it is necessary to integrate only from $\tau = 0$ to $\tau = \pi$, owing to a symmetry property of equations (22) (see Yih & Li 1972; von Kerczek & Davis 1974). The advantages of the above numerical procedure is that all $2M$ sets of equations can be simultaneously integrated and owing to its implicit nature, numerical stability is guaranteed. Characteristic multipliers λ_r of matrix **P** were found using subroutine EIGZC from the IMSL (International Mathematics and Statistics Libraries) package.

To find the critical parameters $\tilde{R}_c$ and a_c, the *regula falsi* and secant root finders were employed along with an interval segmenting minimum finder. The critical values satisfy the relations

$$|\mathrm{Re}\,(\mu(\sigma, a_c, \tilde{R}_c\sqrt{\delta}))| < 10^{-4},$$
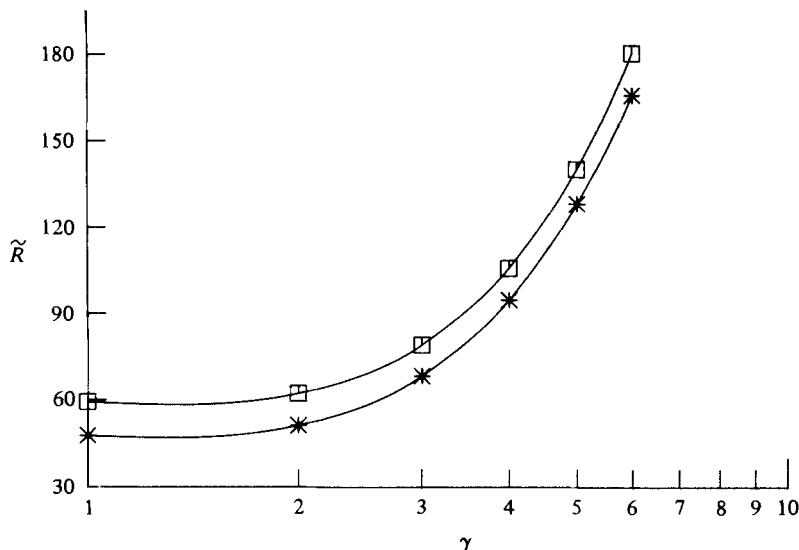$$\tilde{R}_c = \tilde{R}(a_c) = \min\,(\tilde{R}(a)),$$

FIGURE 1. Variation of critical stability parameter $\tilde{R} = (\epsilon_1 R_1 d/\nu)\sqrt{\delta}$ with the modulation frequency $\gamma = [\omega d^2/2\nu]^{\frac{1}{2}}$ for $\Omega_1 = \Omega_2 = \epsilon_2 = 0.$ ✱, gap size $\delta = 0 \cdot 0444$; ☐, $\delta = 0 \cdot 444$.
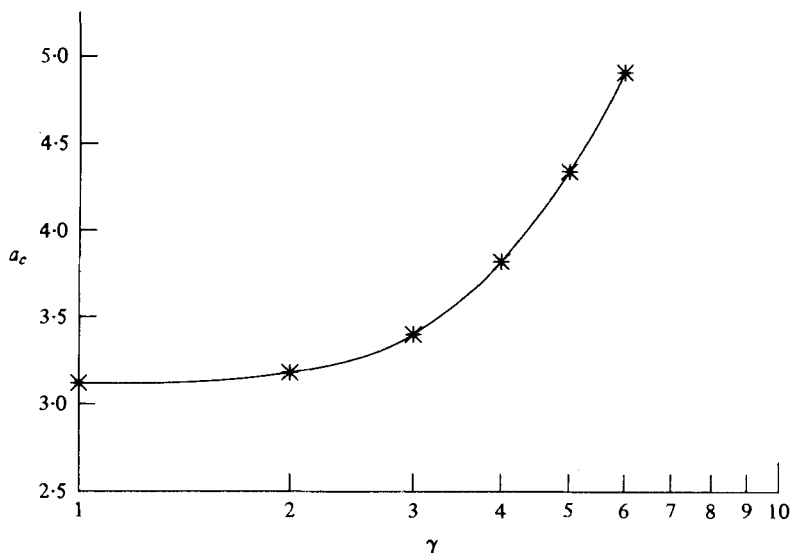

FIGURE 2. Variation of critical wave number a_c with the modulation frequency $\gamma = [\omega d^2/2\nu]^{\frac{1}{2}}$ for $\Omega_1 = \Omega_2 = \epsilon_2 = 0$.

where M, σ and δ were held fixed during the stability limit search. $\tilde{R}$ was found accurately to four significant digits, while a_c can be assumed accurate to the second decimal place. The Galerkin order M needed for convergence of the stability problem varied for different cases (see appendix). This point will be further elaborated in the discussion of the results.

The most time consuming (and therefore most expensive) part of this work is the calculation of the Galerkin coefficients because of the required many evaluations of Bessel functions.

4. Results and discussion

Since in many cases the axisymmetric two-dimensional disturbances ($n = 0$, $k \neq 0$) prove to be the critical ones, we will present these results first and compare them with existing, theoretical and experimental ones in the literature. Results for the two-dimensional case are summarized in tables 1 and 2 and figures 1–9 while the ones for the general three-dimensional non-axisymmetric case ($n \neq 0$, $k \neq 0$) are shown in tables 3 and 4 (comparisons) and figures 10–15.

4.1. *Flows with zero mean rotation subjected to axisymmetric disturbances* ($n = 0$, $k \neq 0$)

We will now consider four cases of modulated Taylor flow about a zero mean ($\Omega_1 = \Omega_2 = 0$):

(a) modulation of the inner cylinder only ($\epsilon_1 \neq 0$, $\epsilon_2 = 0$);

(b) modulation of the outer cylinder only ($\epsilon_1 = 0$, $\epsilon_2 \neq 0$);

(c) modulation of both cylinders with equal amplitude in the same direction ($\epsilon_1/\epsilon_2 = 1\cdot0$); and

(d) modulation of both cylinders with equal amplitude in opposite directions ($\epsilon_1/\epsilon_2 = -1\cdot0$).

Results for the inner cylinder modulation are presented in figures 1 and 2. We took $R_1 = 6\cdot0275$ cm (chosen to compare our results with other investigations) and set $\nu = 1$, where R_1 and ν are the inner radius and kinematic viscosity, respectively. Here a_c, the critical axial wavenumber, corresponds to the minimum Taylor number $\tilde{R} = (\epsilon_1 R_1 d/\nu)\sqrt{\delta}$, where $\delta = d/R_1$. We will limit our studies to two values for δ, $0\cdot0444$ and $0\cdot444$, the former for purposes of comparison with other investigations and the latter as a convenient wide-gap value. The non-dimensional frequency parameter $\gamma = (\omega d^2/2\nu)^{\frac{1}{2}}$ (equivalent Stokes-layer thickness) was varied over a reasonable range from $1\cdot0$ to $6\cdot0$. The Galerkin series expansion order M needed for convergence was found to be higher for larger values of γ, but for $\gamma < 4$, $M = 3$ was found to be adequate. Convergence was assumed when $\tilde{R}$ corresponding to order M was within 2% of the one corresponding to order $M + 1$ (see appendix),

$$\left| \frac{\tilde{R}_M - \tilde{R}_{M+1}}{\tilde{R}_M} \right| < 0\cdot02.$$

The two curves in figure 1 represent two different gap sizes, $0\cdot0444$ and $0\cdot444$. Although the larger gap has a higher critical Taylor number, the qualitative behaviour of the two curves is identical. For $\gamma \to 0$ the critical Taylor number $\tilde{R}$ approaches $\tilde{R}_0$ (the steady-flow stability limit), while it increases monotonically for $\gamma \to \infty$. This behaviour occurs because at higher frequencies the magnitude of velocity decreases rapidly with distance away from the inner cylinder wall thus becoming essentially only a boundary-layer effect. The effect of gap size on a_c is almost negligible. In figure 2 we plotted a_c versus γ. As $\gamma \to 0$, a_c again approaches the limiting value for steady flow, whereas for $\gamma \to \infty$ it increases monotonically with γ. Both $\tilde{R}$ and a_c were found to be smooth continuous functions of γ.

Thompson (1968) solved the zero mean inner cylinder modulation problem using finite differences and then performed laboratory experiments for verification. In his
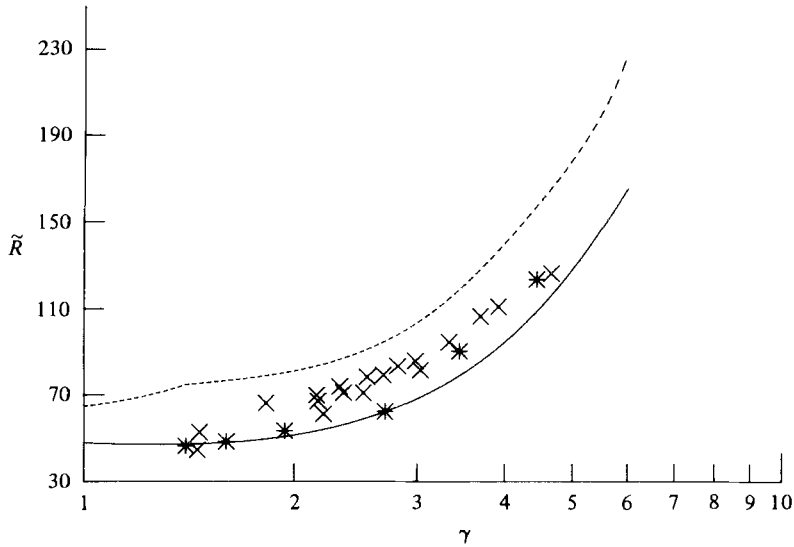
FIGURE 3. Comparison of current results with other investigations for $\Omega_1 = \Omega_2 = \epsilon_2 = 0$ and gap size $\delta = 0.0444$ ($\tilde{R} = (\epsilon_1 R_1 d/\nu)\sqrt{\delta}, \gamma = [\omega d^2/2\nu]^{\frac{1}{2}}$): ——, our results; ✳, Thompson's theoretical results; ×, Thompson's experimental data; – – –, results from Riley & Laurence for $\delta \to 0$.

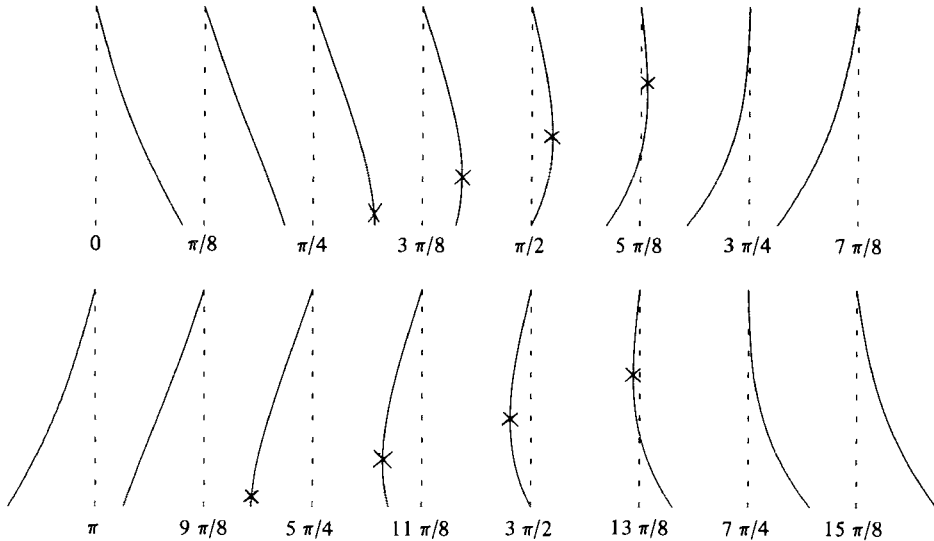FIGURE 4. Evolution of the basic velocity profile over one period for gap size $\delta = 0.0444$, frequency $\gamma = 1.5$, and $\Omega_1 = \Omega_2 = \epsilon_2 = 0$. × 's denote points where $D * V \to 0$ and V/r remains finite.

theoretical and experimental investigation he took $R_1 = 6.0275$ cm and $\delta = 0.0444$. Riley & Laurence (1976) solved the same problem in the small-gap approximation (neglecting terms of order δ) and used the Galerkin method along with the Floquet theory. Figure 3 shows a comparison of our results with the ones obtained by the above investigators. The solid line represents the lower curve of figure 1, while the × 's are points at which Thompson experimentally observed instability through flow
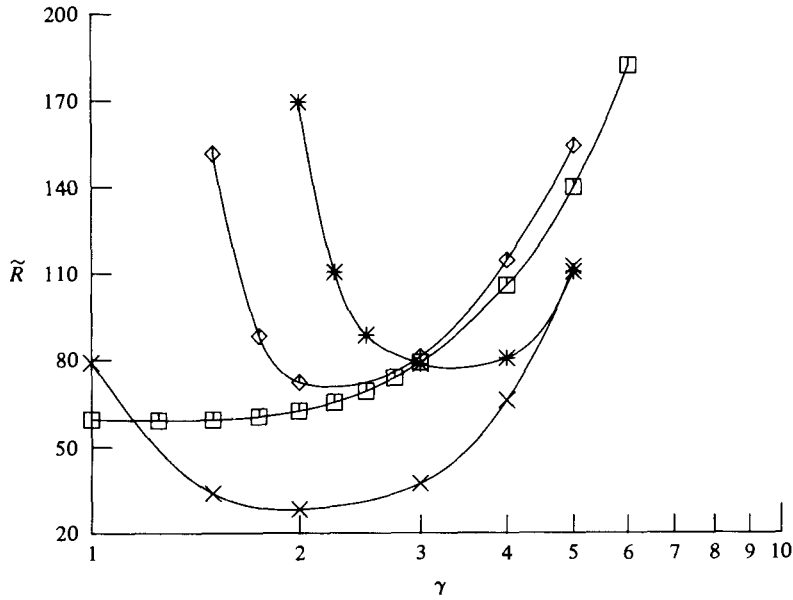
FIGURE 5. Zero mean modulation with gap size $\delta = 0\cdot444$. $\tilde{R} = (\epsilon_2 R_2 d/\nu)\sqrt{\delta}$ for $\epsilon_2 \neq 0$ and $\epsilon_1 = 0$, otherwise $\tilde{R} = (\epsilon_1 R_1 d/\nu)\sqrt{\delta}$. $\times$, $\epsilon_1/\epsilon_2 = 1\cdot0$; $\square$, $\epsilon_2 = 0$; $\diamondsuit$, $\epsilon_1 = 0$; $*$, $\epsilon_1/\epsilon_2 = -1\cdot0$.

γ	M	a_c	$\tilde{R}$	Type
$1\cdot00$	4	$3\cdot12$	$59\cdot42$	$\epsilon_2 = 0$
$2\cdot00$	4	$3\cdot18$	$62\cdot38$	$\epsilon_2 = 0$
$3\cdot00$	4	$3\cdot40$	$79\cdot08$	$\epsilon_2 = 0$
$4\cdot00$	4	$3\cdot82$	$105\cdot6$	$\epsilon_2 = 0$
$5\cdot00$	4	$4\cdot34$	$139\cdot9$	$\epsilon_2 = 0$
$6\cdot00$	6	$4\cdot91$	$178\cdot0$	$\epsilon_2 = 0$
$1\cdot50$	3	$3\cdot57$	$151\cdot6$ (h)	$\epsilon_1 = 0$
$1\cdot75$	3	$3\cdot08$	$88\cdot13$	$\epsilon_1 = 0$
$2\cdot00$	4	$3\cdot13$	$72\cdot16$	$\epsilon_1 = 0$
$3\cdot00$	4	$3\cdot29$	$80\cdot99$	$\epsilon_1 = 0$
$4\cdot00$	4	$3\cdot74$	$114\cdot3$	$\epsilon_1 = 0$
$5\cdot00$	4	$4\cdot35$	$154\cdot2$	$\epsilon_1 = 0$
$1\cdot00$	3	$3\cdot37$	$79\cdot01$ (h)	$\epsilon_1/\epsilon_2 = 1\cdot0$
$1\cdot50$	3	$3\cdot10$	$33\cdot74$	$\epsilon_1/\epsilon_2 = 1\cdot0$
$2\cdot00$	3	$3\cdot12$	$28\cdot17$	$\epsilon_1/\epsilon_2 = 1\cdot0$
$3\cdot00$	3	$3\cdot12$	$37\cdot23$	$\epsilon_1/\epsilon_2 = 1\cdot0$
$4\cdot00$	3	$3\cdot22$	$65\cdot91$	$\epsilon_1/\epsilon_2 = 1\cdot0$
$5\cdot00$	4	$4\cdot10$	$113\cdot1$	$\epsilon_1/\epsilon_2 = 1\cdot0$
$2\cdot00$	3	$4\cdot21$	$169\cdot5$ (h)	$\epsilon_1/\epsilon_2 = -1\cdot0$
$2\cdot25$	3	$3\cdot41$	$110\cdot3$	$\epsilon_1/\epsilon_2 = -1\cdot0$
$2\cdot50$	3	$3\cdot64$	$88\cdot51$	$\epsilon_1/\epsilon_2 = -1\cdot0$
$3\cdot00$	3	$3\cdot82$	$78\cdot51$	$\epsilon_1/\epsilon_2 = -1\cdot0$
$4\cdot00$	3	$4\cdot05$	$80\cdot45$	$\epsilon_1/\epsilon_2 = -1\cdot0$
$5\cdot00$	4	$4\cdot24$	$97\cdot29$	$\epsilon_1/\epsilon_2 = -1\cdot0$

(h) denotes half frequency response.

TABLE 1. Modulation about a zero mean ($\Omega_1 = \Omega_2 = 0$) for gap size $\delta = 0\cdot444$.

visualization. Thompson's theoretical results are depicted as *'s and the broken line is the stability boundary obtained by Riley & Laurence. Excellent agreement is found between our results and Thompson's theoretical ones, while Riley & Laurence's figures are somewhat higher. The discrepancy with the latter can be partially explained by their approximation of the term $D * V + V/\beta$ by $D * V$ in (12). This approximation, although valid for the steady state, cannot be justified for the unsteady case. To illustrate this, one can look at the evolution of the velocity profile over one period for $\gamma = 1.5$, as shown in figure 4. This is exactly the frequency at which Riley & Laurence predict a discontinuity in a_c along with a derivative discontinuity for $\tilde{R}$. The ×'s in figure 4 indicate points on the velocity profile where the value $D * V$ approaches zero while V/β remains finite. Further discussion on this matter can be found in the appendix.

For cases (b), (c) and (d), listed on page 27, we found a considerable similarity in behaviour which is, however, markedly different from that of inner cylinder modulation (see figure 5 and table 1). The critical Taylor number is defined as before except for the cases with outer modulation only, where $\tilde{R} = (\epsilon_2 R_2 d/\nu)\sqrt{\delta}$. We found that $\tilde{R}$ reached a minimum in the range $\gamma = 2.0\text{--}3.0$ and approaches infinity as $\gamma \to 0$ or $\gamma \to \infty$. For small γ the response is no longer synchronous but at half the frequency of the boundary oscillation. Table 1 and figure 5 illustrate the functional relationship between $\tilde{R}$ and γ for all 4 cases with $\delta = 0.444$. Modulation of both cylinders in phase is the most destabilizing, while out of phase is the least.

The mechanism of instability for the above mentioned cases can partially be explained by examining the time evolution of a velocity profile over one period of zero-mean rotation of the outer cylinder. At some time during the cycle, Rayleigh's (1920) inviscid criterion is clearly violated and when the amplitude is sufficiently large, the viscous forces will be overtaken and centrifugal instability will occur. This result is definitely different than the one obtained for steady rotation of the outer cylinder only, where the angular momentum increases monotonically outward, and the flow is therefore stable by Rayleigh's criterion.

4.2. *Flows with non-zero mean rotation subjected to axisymmetric disturbances* $(n = 0, k \neq 0)$

The results for the non-zero mean modulation problem are given in figures 6–8 and table 2. In these cases, the steady component of the flow had the inner cylinder rotating, while the outer remained at rest ($\Omega_1 \neq 0$, $\Omega_2 = 0$). Figures 6 and 7 show the relationship of $\tilde{R} = (\Omega_1 R_1 d/\nu)\sqrt{\delta}$ and a_c, respectively, versus γ for amplitude ratio $\epsilon_1/\Omega_1 = 5.0$. Again, as in the zero-mean case, $\tilde{R}$ is higher for $\delta = 0.444$ than for $\delta = 0.0444$. The results for $\epsilon_1/\Omega_1 = 0.5$, $\epsilon_2 = 0$ and $\delta = 0.444$ are given in table 2 and figure 8. In general we found that the qualitative behaviour of $\tilde{R}$ and a_c versus γ is independent of δ and the amplitude ratio. In the limit as $\gamma \to 0$, $\tilde{R}$ approaches $\tilde{R}_0 \Omega_1/(\Omega_1 + \epsilon_1)$, where $\tilde{R}_0$ is the stability limit for $\Omega_1 \neq 0$, $\epsilon_1 = 0$ (steady rotation of the inner cylinder). We found $\tilde{R}$ to be less than $\tilde{R}_0$ for all γ; however, $\tilde{R}$ approaches $\tilde{R}_0$ asymptotically as $\gamma \to \infty$. For $\gamma \to 0$ or $\gamma \to \infty$ we found a_c to equal a_{c0} (critical wavenumber for steady flow), while reaching a maximum near $\gamma = 7.0$. Both $\tilde{R}$ and a_c are smooth continuous functions of γ and the response is synchronous everywhere.

Hall (1975) and Riley & Laurence (1976) have investigated theoretically the non-zero-mean modulation of the inner cylinder. Hall solved this problem for the small-
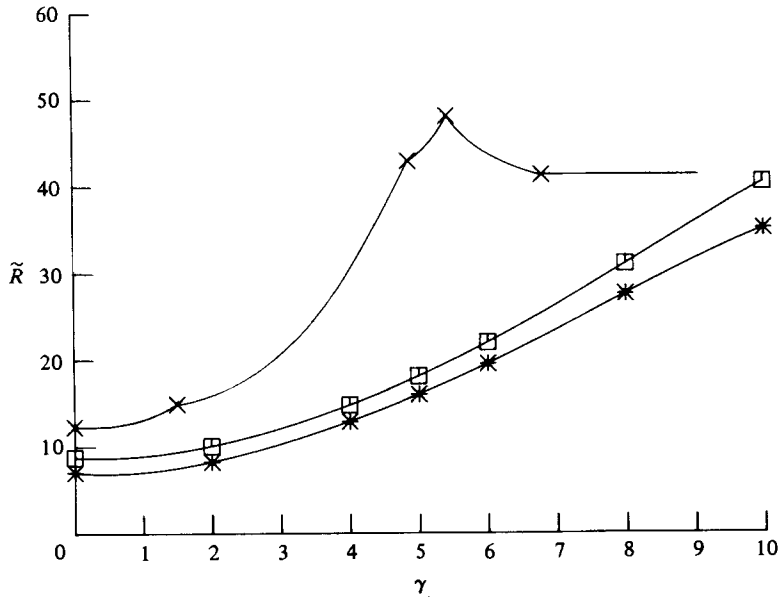
FIGURE 6. Critical parameters $\widetilde{R} = (\Omega_1 R_1 d/\nu)\sqrt{\delta}$ versus frequency γ for $\Omega_2 = \epsilon_2 = 0$ and $\epsilon_1/\Omega_1 = 5\cdot0$: ⊡, gap size $\delta = 0\cdot444$; ✳, $\delta = 0\cdot0444$; ×, results from Riley & Laurence for $\delta \to 0$.

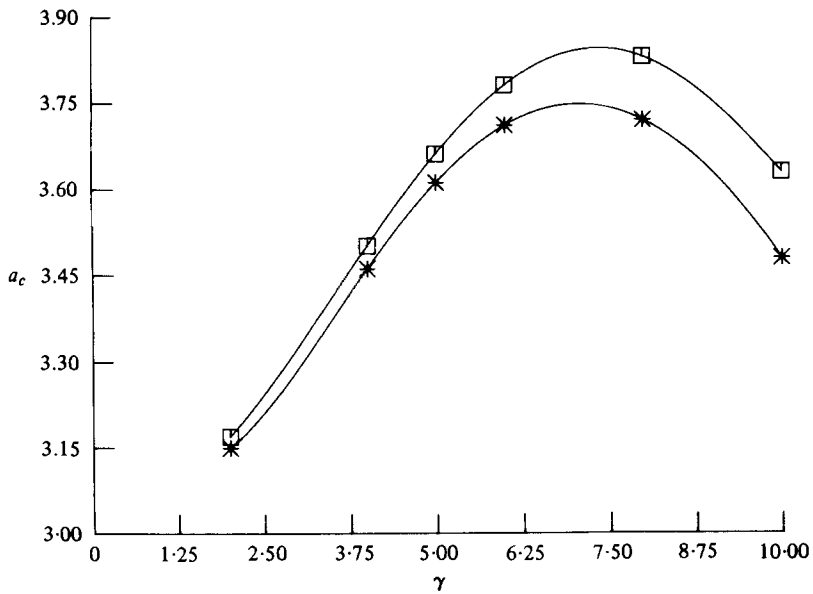

FIGURE 7. Critical wave number a_c versus frequency γ for $\Omega_2 = \epsilon_2 = 0$ and $\epsilon_1/\Omega_1 = 5\cdot0$: ⊡, $\delta = 0\cdot444$; ✳, $\delta = 0\cdot0444$.

γ	M	a_c	$\tilde{R}$	Type
1·0	3	3·13	36·42	$\epsilon_1/\Omega_1 = 0·5,\ \epsilon_2 = 0$
2·0	3	3·15	36·89	$\epsilon_1/\Omega_1 = 0·5,\ \epsilon_2 = 0$
4·0	3	3·21	41·30	$\epsilon_1/\Omega_1 = 0·5,\ \epsilon_2 = 0$
5·0	3	3·22	43·88	$\epsilon_1/\Omega_1 = 0·5,\ \epsilon_2 = 0$
6·0	3	3·22	46·25	$\epsilon_1/\Omega_1 = 0·5,\ \epsilon_2 = 0$
8·0	3	3·19	49·61	$\epsilon_1/\Omega_1 = 0·5,\ \epsilon_2 = 0$
10·0	3	3·17	51·26	$\epsilon_1/\Omega_1 = 0·5,\ \epsilon_2 = 0$
1·0	3	3·12	48·91	$\epsilon_2/\Omega_1 = 0·5,\ \epsilon_1 = 0$
2·0	3	3·12	34·51	$\epsilon_2/\Omega_1 = 0·5,\ \epsilon_1 = 0$
4·0	3	3·11	40·50	$\epsilon_2/\Omega_1 = 0·5,\ \epsilon_1 = 0$
5·0	3	3·10	44·73	$\epsilon_2/\Omega_1 = 0·5,\ \epsilon_1 = 0$
6·0	3	3·10	48·08	$\epsilon_2/\Omega_1 = 0·5,\ \epsilon_1 = 0$
8·0	3	3·11	51·61	$\epsilon_2/\Omega_1 = 0·5,\ \epsilon_1 = 0$
10·0	3	3·12	52·47	$\epsilon_2/\Omega_1 = 0·5,\ \epsilon_1 = 0$
1·0	3	3·12	33·92	$\epsilon_1/\Omega_1 = 0·5,\ \epsilon_1/\epsilon_2 = 1·0$
2·0	3	3·12	27·11	$\epsilon_1/\Omega_1 = 0·5,\ \epsilon_1/\epsilon_2 = 1·0$
4·0	3	3·13	34·73	$\epsilon_1/\Omega_1 = 0·5,\ \epsilon_1/\epsilon_2 = 1·0$
5·0	3	3·14	39·58	$\epsilon_1/\Omega_1 = 0·5,\ \epsilon_1/\epsilon_2 = 1·0$
6·0	3	3·15	43·66	$\epsilon_1/\Omega_1 = 0·5,\ \epsilon_1/\epsilon_2 = 1·0$
8·0	3	3·16	49·96	$\epsilon_1/\Omega_1 = 0·5,\ \epsilon_1/\epsilon_2 = 1·0$
10·0	3	3·15	51·26	$\epsilon_1/\Omega_1 = 0·5,\ \epsilon_1/\epsilon_2 = 1·0$
1·0	3	3·22	45·62	$\epsilon_1/\Omega_1 = 0·5,\ \epsilon_1/\epsilon_2 = -1·0$
2·0	3	3·12	47·32	$\epsilon_1/\Omega_1 = 0·5,\ \epsilon_1/\epsilon_2 = -1·0$
3·0	3	3·13	45·05	$\epsilon_1/\Omega_1 = 0·5,\ \epsilon_1/\epsilon_2 = -1·0$
4·0	3	3·13	47·75	$\epsilon_1/\Omega_1 = 0·5,\ \epsilon_1/\epsilon_2 = -1·0$
6·0	3	3·09	52·75	$\epsilon_1/\Omega_1 = 0·5,\ \epsilon_1/\epsilon_2 = -1·0$
7·0	3	3·07	53·92	$\epsilon_1/\Omega_1 = 0·5,\ \epsilon_1/\epsilon_2 = -1·0$
8·0	3	3·08	54·19	$\epsilon_1/\Omega_1 = 0·5,\ \epsilon_1/\epsilon_2 = -1·0$
10·0	3	3·10	53·65	$\epsilon_1/\Omega_1 = 0·5,\ \epsilon_1/\epsilon_2 = -1·0$

TABLE 2. Modulation about a non-zero mean ($\Omega_2 = 0$) for gap size $\delta = 0·444$.

gap approximation using perturbation techniques. He found that as $\epsilon_1/\Omega_1 \to 0$ with $\gamma^2\Omega_1/\epsilon_1$ constant, $\tilde{R} = \tilde{R}_0 - O(\epsilon_1^2/\Omega_1^2) + O(\epsilon_1^2\gamma^4/\Omega_1^2) + \dots$. In the limit, as $\gamma \to \infty$ with ϵ_1/Ω_1 arbitrary, he found $\tilde{R}$ to be less than $\tilde{R}_0$ by order $\epsilon_1^2/\Omega_1^2\gamma^6$. Riley & Laurence also solved this problem for the small-gap approximation using the Galerkin method coupled with Floquet theory. For small ϵ_1/Ω_1 their results are in good agreement with ours and those of Hall. For larger ϵ_1/Ω_1, however, their results contrast ours. A comparison of our results with those of Riley & Laurence are shown in figure 6. The discrepancy can again, as in the zero-mean case, be partially explained by the fact that approximating $D * V + V/\beta$ by $D * V$ in equation (12) is not justified for unsteady flows. The error is small for $\epsilon_1/\Omega_1 \ll 1$; but is becoming more pronounced for larger ϵ_1/Ω_1. We studied a few cases without the V/β term and our results changed in the direction of Riley & Laurence. Part of the discrepancy is probably also due to their using Cartesian rather than cylindrical operators and therefore neglecting some potentially important terms.

Seminara & Hall (1976), in commenting on their results, show a functional relationship between $\tilde{R}$ and γ which is similar to the one obtained by Riley & Laurence (see figure 6). Since Seminara & Hall use the thin boundary-layer approximation which is essentially the same as using Riley & Laurence's small-gap approximation, it is
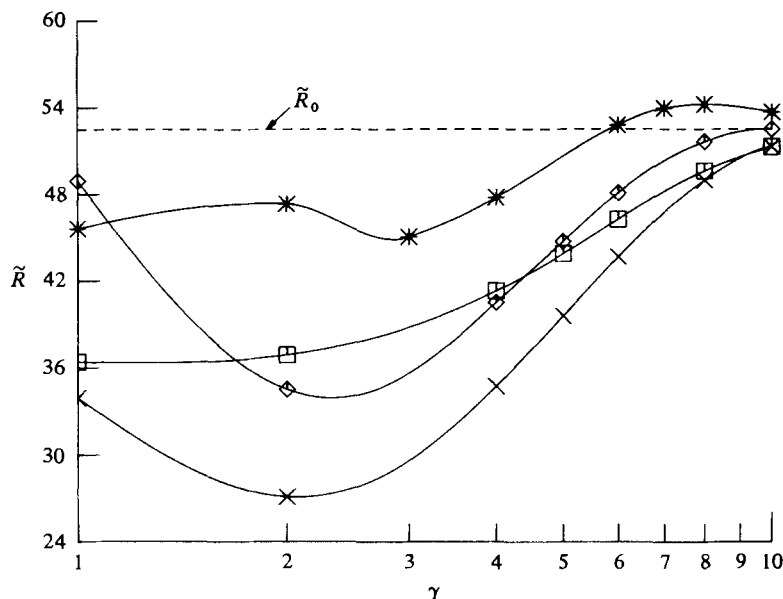
FIGURE 8. Critical parameter $\tilde{R} = (\Omega_1 R_1 d/\nu)\sqrt{\delta}$ versus frequency γ for $\Omega_2 = 0$ and $\delta = 0.444$: X, $\epsilon_1/\epsilon_2 = 1.0$ and $\epsilon_1/\Omega_1 = 0.5$; $\diamondsuit$, $\epsilon_1 = 0$ and $\epsilon_2/\Omega_1 = 0.5$; $*$, $\epsilon_1/\epsilon_2 = -1.0$ and $\epsilon_1/\Omega_1 = 0.5$; $\square$, $\epsilon_2 = 0$ and $\epsilon_1/\Omega_1 = 0.5$.

reasonable to assume that their results are subject to the same errors as pointed out earlier (see appendix for more details).

Laboratory experiments have been performed by both Donnelly (1964) and Thompson (1968). Thompson states that the flow becomes unstable when

$$\tilde{R} > \tilde{R}_0\,\Omega_1/(\Omega_1 + \epsilon_1)$$

for $\gamma \to 0$ or when $\tilde{R} > \tilde{R}_0$ for $\gamma \to \infty$. This agrees with our findings. Donnelly, on the other hand, reported that for $\epsilon_1/\Omega_1 \leqslant 0.25$ and small γ, $\tilde{R} > \tilde{R}_0$. His experimental criterion for stability was not the absence of vortex motion but the requirement that the amplitude of radial perturbations integrated over one period should remain constant. Donnelly, however, documented the appearance of 'transient vortices' below his critical $\tilde{R}$ and if the onset of these vortices is taken as the stability limit, our results may compare more favourably with his. Similar interpretations of Donnelly's experiments have been offered by Thompson, Hall and Riley & Laurence.

Figure 8 and table 2 show the results for four cases where $\delta = 0.444$ and the modulation amplitude is one half that of the steady-flow angular velocity. We found that for outer cylinder modulation ($\epsilon_2/\Omega_1 = 0.5$, $\epsilon_1 = 0$), $\tilde{R}$ reached a minimum in the range of $\gamma = 2.0$–3.0 and approached $\tilde{R}_0$ as $\gamma \to \infty$. For $\gamma \to 0$, weak stabilization ($\tilde{R} > \tilde{R}_0$) is realized. Modulation of both cylinders in phase ($\epsilon_1/\Omega_1 = 0.5$, $\epsilon_1/\epsilon_2 = 1.0$) was found to be destabilizing for all γ with $\tilde{R}$ reaching a minimum near $\gamma = 2.0$ and approaching $\tilde{R}_0$ as $\gamma \to \infty$. Modulation of both cylinders in opposite directions shows the most interesting behaviour. $\tilde{R}$ has a local maximum near $\gamma = 8.0$ and as $\gamma \to \infty$, $\tilde{R} \to \tilde{R}_0$ from above. A local minimum was found near $\gamma = 3.0$ and another local maximum near $\gamma = 2.0$. In the two cases where both cylinders are modulated, when $\gamma \to 0$, $\tilde{R}$ approaches a finite value less than $\tilde{R}_0$ and there is some evidence, although inconclusive, that this value may also be $\tilde{R}_0\Omega_1/(\Omega_1 + \epsilon_1)$.
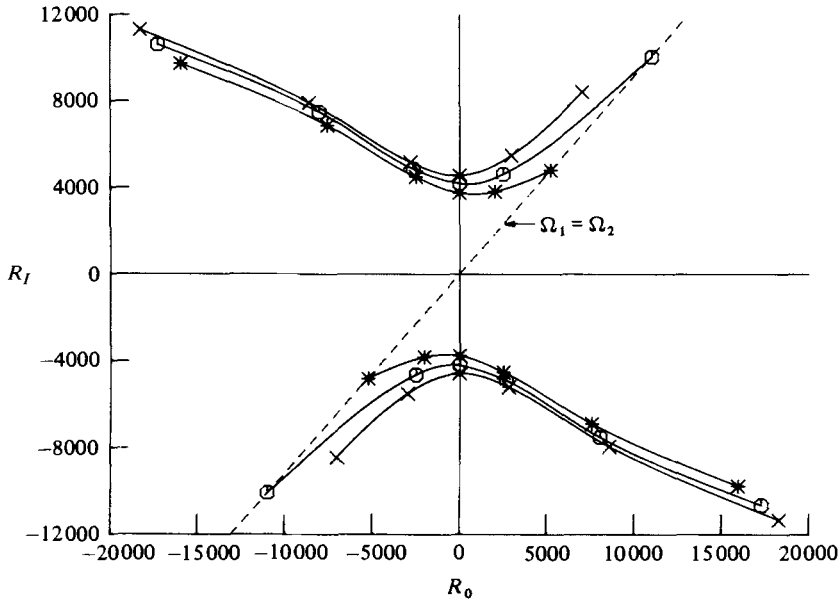
FIGURE 9. Linear stability boundary for different degrees of modulation amplitude, gap size $\delta = 0.0444$, $R_I = \Omega_1 R_1^2/\nu$ and $R_0 = \Omega_2 R_2^2/\nu$: $\times$, 0% modulation (steady); $\bigcirc$, 10% modulation ($\epsilon_1/\Omega_1 = \epsilon_2/\Omega_2 = 0.1$); $*$, 25% modulation ($\epsilon_1/\Omega_1 = \epsilon_2/\Omega_2 = 0.25$).

In figure 9 we show the stability boundaries for modulation about a non-zero mean, where Ω_2 is not necessarily equal to zero ($\Omega_1 \neq 0$, $\Omega_2 \neq 0$). As critical parameters we use two Reynolds numbers $R_I = \Omega_1 R_1^2/\nu$ and $R_0 = \Omega_2 R_2^2/\nu$ and the amplitude ratio of modulation to mean rotation is held constant, i.e. $\epsilon_1/\Omega_1 = \epsilon_2/\Omega_2$. The plot shows a comparison between 10 and 25 % modulation with the stability boundary for the steady case. Again we see that modulation in phase is more destabilizing than out of phase and that the qualitative behaviour does not change with amplitude.

4.3. *Flows subjected to general three-dimensional disturbances*
$$(n \neq 0, k \neq 0)$$

At first, as a numerical check, we used our formulation to study the instability of steady Taylor flow due to general three-dimensional disturbances. Krueger, Gross & Diprima (1966) analytically determined that for the case $\Omega_2/\Omega_1 = -1.0$, $R_1/R_2 = 0.95$ the critical azimuthal wavenumber is $n = 4$. We examined this case using our formulation and the critical rotational speeds and axial wavenumbers that we obtained were in agreement with theirs. We then extended Krueger *et al.*'s results to other configurations of steady basic flows. One such example is shown in figure 10, where we chose the gap size $\delta = 0.135$. The solid line in figure 10 represents the stability boundary for $n = 0$, while the circles represent critical angular velocities obtained for general non-axisymmetric disturbances. This configuration has been studied experimentally by Coles (1965), who observed a weak helical flow structure near the stability boundary for $\Omega_2/\Omega_1 = -1.0$ but described a catastrophic transition to turbulence for decreasing values of Ω_2/Ω_1. Since our results agreed both quantitatively and qualitatively with the ones obtained by Coles and Krueger *et al.*, we proceeded with our stability analysis of unsteady flows.
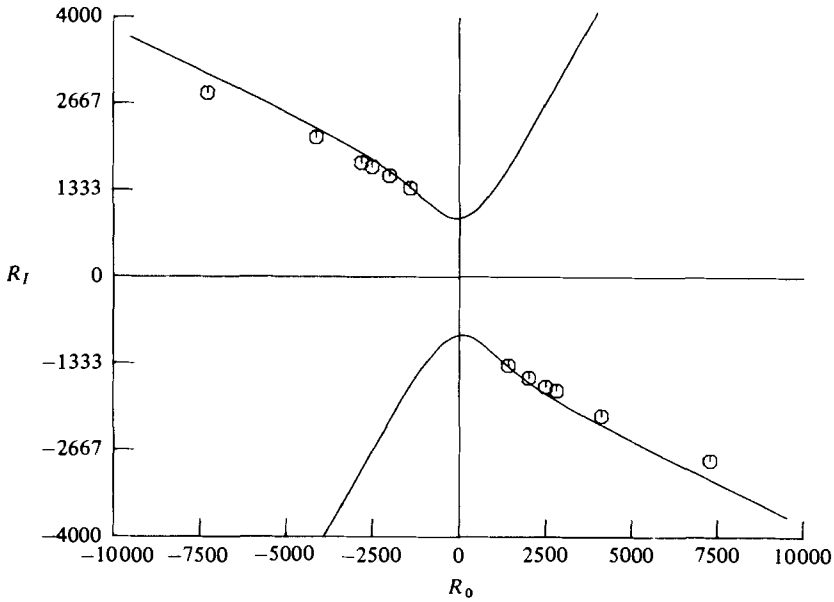
FIGURE 10. Stability boundary for $\epsilon_2 = \epsilon_1 = 0\cdot0$ (steady) and gap size $\delta = 0\cdot135$. The critical parameters are: $R_0 \equiv \Omega_2 R_2^2/\nu$ and $R_I \equiv \Omega_1 R_1^2/\nu$. ——, Taylor boundary for axisymmetric disturbances; $\bigcirc$, the Krueger mode.
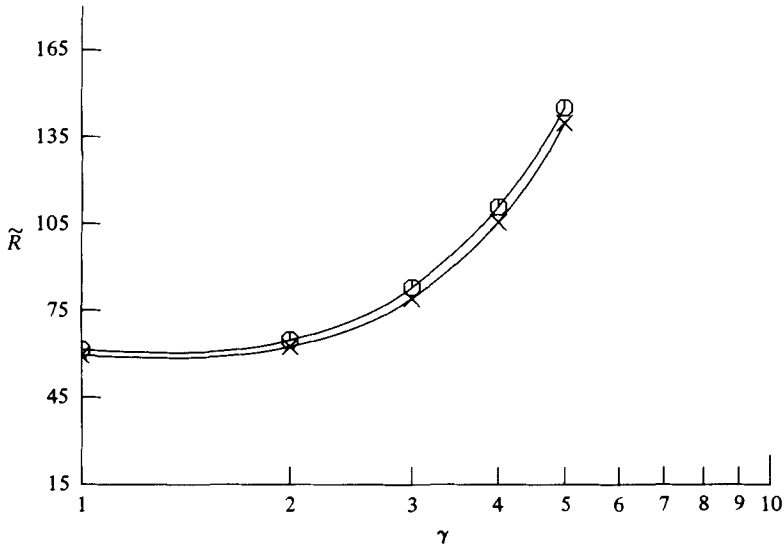

FIGURE 11. Critical parameter $\tilde{R} = (\epsilon_1 R_1 d/\nu)\sqrt{\delta}$ versus frequency γ for $\Omega_1 = \Omega_2 = \epsilon_2 = 0$ and gap size $\delta = 0\cdot444$: $\times, n = 0$; $\bigcirc, n = 1$.

The evaluation of critical parameters for unsteady basic flows with arbitrary three-dimensional disturbances generally requires a considerable amount of computer time. We found that the critical axial wavenumber a_c does not change substantially between $n = 0$ and $n = 1$, and therefore, we evaluated the stability limits for wavenumber $n = 1$, while setting the axial wavenumber a equal to the critical one found for axisymmetric disturbances. Although this procedure did not yield the critical azimuthal
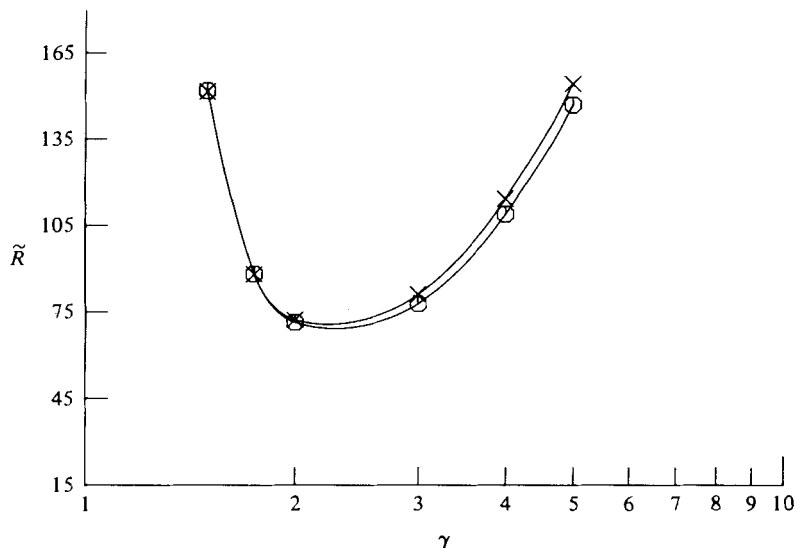
FIGURE 12. Critical parameter $\tilde{R} = (\epsilon_2 R_2 d/\nu)\sqrt{\delta}$ versus frequency γ for
$\Omega_1 = \Omega_2 = \epsilon_1 = 0$ and gap size $\delta = 0.444$: $\times$, $n = 0$; $\bigcirc$, $n = 1$.

FIGURE 13. Critical parameter $\tilde{R} = (\epsilon_1 R_1 d/\nu)\sqrt{\delta}$ versus frequency γ for
$\Omega_1 = \Omega_2 = 0$, $\epsilon_1 = \epsilon_2$ and gap size $\delta = 0.444$: $\times$, $n = 0$; $\bigcirc$, $n = 1$.

wavenumber n_c, we did however determine the cases where the three-dimensional
non-axisymmetric disturbances are more critical than the two-dimensional axi-
symmetric ones.

Figures 11–14 and table 3 give a comparison of the stability limits between wave-
numbers $n = 0$ and $n = 1$ for modulation about a zero mean. For sinusoidal motion
of the inner cylinder (see figure 11) the stability limit for $n = 1$ is higher than the one
for $n = 0$ for all frequencies and we conclude, therefore, that the critical disturbances
are two-dimensional and axisymmetric. These results are consistent with Thompson's
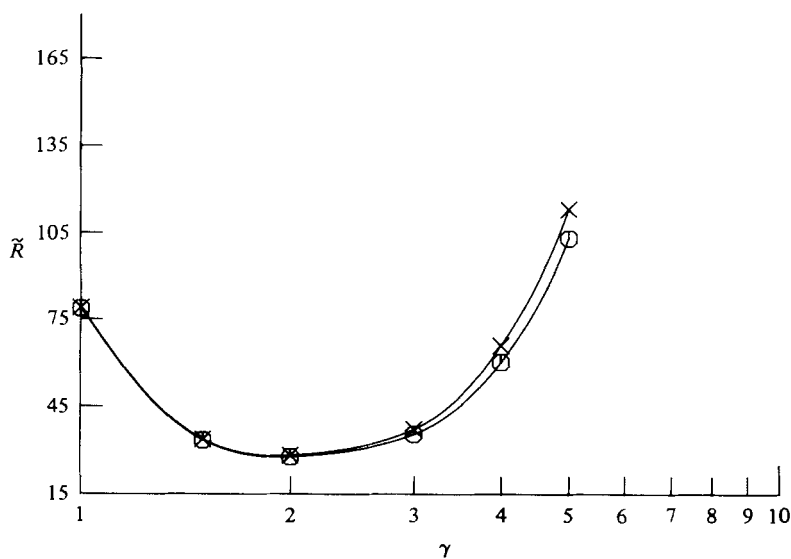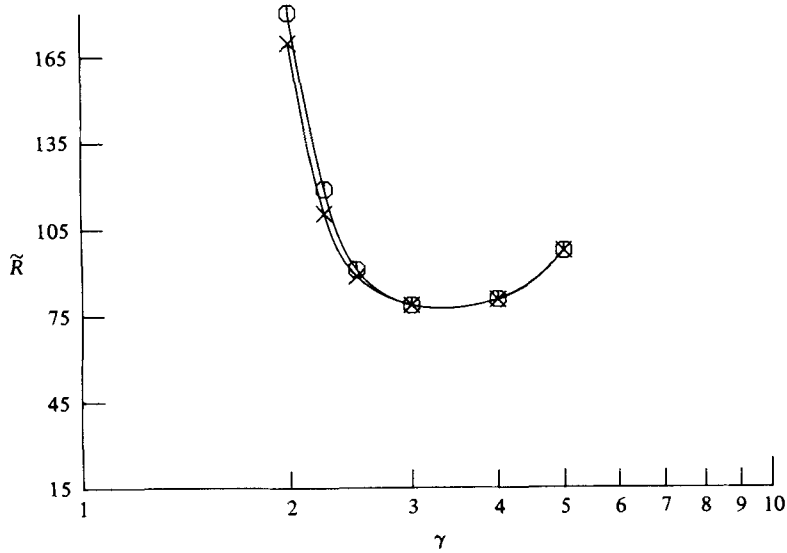
FIGURE 14. Critical parameter $\tilde{R} = (\epsilon_1 R_1 d/\nu)\sqrt{\delta}$ versus frequency γ for $\Omega_1 = \Omega_2 = 0$, $\epsilon_1 = -\epsilon_2$ and gap size $\delta = 0.444$: $\times$, $n = 0$; $\bigcirc$, $n = 1$.

γ	M	a	$\tilde{R}$ ($n = 0$)	$\tilde{R}$ ($n = 1$)	Type
1·00	4	3·12	59·42	61·367	$\epsilon_2 = 0$
2·00	4	3·18	62·38	64·621	$\epsilon_2 = 0$
3·00	4	3·40	79·08	82·930	$\epsilon_2 = 0$
4·00	4	3·82	105·6	110·89	$\epsilon_2 = 0$
5·00	4	4·34	139·9	145·29	$\epsilon_2 = 0$
1·50	3	3·57	151·6	151·81	$\epsilon_1 = 0$
1·75	3	3·08	88·13	88·193	$\epsilon_1 = 0$
2·00	4	3·13	72·16	71·318	$\epsilon_1 = 0$
3·00	4	3·29	80·99	77·820	$\epsilon_1 = 0$
4·00	4	3·74	114·3	108·89	$\epsilon_1 = 0$
5·00	4	4·35	154·2	146·92	$\epsilon_1 = 0$
1·00	3	3·37	79·01	78·696	$\epsilon_1 = \epsilon_2$
1·50	3	3·10	33·74	33·430	$\epsilon_1 = \epsilon_2$
2·00	3	3·12	28·17	27·673	$\epsilon_1 = \epsilon_2$
3·00	3	3·12	37·23	35·486	$\epsilon_1 = \epsilon_2$
4·00	3	3·22	65·91	60·180	$\epsilon_1 = \epsilon_2$
5·00	4	4·10	113·1	103·00	$\epsilon_1 = \epsilon_2$
2·00	3	4·21	169·5	179·98	$\epsilon_1 = -\epsilon_2$
2·25	3	3·41	110·3	118·67	$\epsilon_1 = -\epsilon_2$
2·50	3	3·64	88·51	90·833	$\epsilon_1 = -\epsilon_2$
3·00	3	3·82	78·51	78·467	$\epsilon_1 = -\epsilon_2$
4·00	3	4·05	80·45	80·610	$\epsilon_1 = -\epsilon_2$
5·00	4	4·24	97·29	97·273	$\epsilon_1 = -\epsilon_2$

TABLE 3. Comparison of the linear stability limit for $n = 0$ *vs.* $n = 1$ for modulation about a zero mean ($\Omega_1 = \Omega_2 = 0$) and gap size $\delta = 0.444$.

γ	a	$\tilde{R}\ (n = 0)$	$\tilde{R}\ (n = 1)$
1·0	3·22	45·62	48·758
2·0	3·12	47·32	63·670
3·0	3·13	45·05	59·965
4·0	3·13	47·75	52·728
6·0	3·09	52·75	50·478
7·0	3·07	53·92	51·139
8·0	3·08	54·19	51·838
10·0	3·10	53·65	52·944

TABLE 4. Comparison of linear stability limit for $n = 0$ *vs.* that for $n = 1$ with gap size $\delta = 0\cdot444$, $M = 3$, $\Omega_2 = 0$ and $\epsilon_1/\Omega_1 = -\epsilon_2/\Omega_1 = 0\cdot5$.
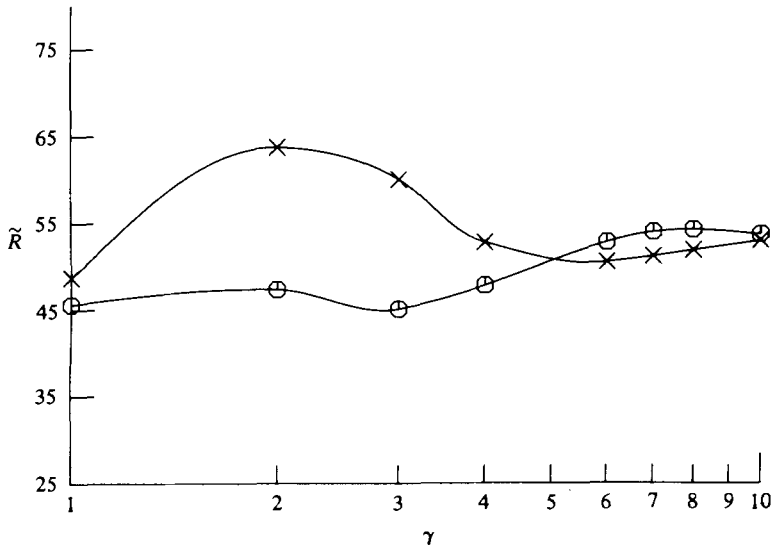

FIGURE 15. Critical parameter $\tilde{R} = (\Omega_1 R_1 d/\nu)\sqrt{\delta}$ versus frequency γ for $\Omega_2 = 0$, $\epsilon_1/\Omega_1 = -\epsilon_2/\Omega_1 = 0\cdot5$ and gap size $\delta = 0\cdot444$: $\times$, $n = 1$; $\bigcirc$, $n = 0$.

(1968), who observed only axisymmetric secondary motion in his experimental work. For modulation of the outer cylinder (see figure 12), the results differ. At low frequencies, the critical disturbances are axisymmetric; however, near $\gamma = 2\cdot0$ the stability limit for $n = 1$ falls below the limit for $n = 0$ and remains so for higher frequencies. For modulation of both cylinders in phase (see figure 13) we found that the $n = 1$ curve falls below the $n = 0$ curve for all frequencies studied and the difference widens with γ increasing. For both cylinders oscillating in opposite directions (see figure 14) the critical disturbances remain axisymmetric until $\gamma = 5\cdot0$ is reached.

Table 4 and figure 15 give a comparison of the stability limits for $n = 0$ and $n = 1$ for a non-zero-mean modulation, where $\epsilon_1/\Omega_1 = -\epsilon_2/\Omega_1 = 0\cdot5$ and $\Omega_2 = 0$. At low frequencies the $n = 1$ limit is considerable higher than for the $n = 0$ curve; however, for $\gamma > 5\cdot0$ the response is no longer axisymmetric. The results for this case clearly indicate that the possibility of stabilization at higher frequencies only occurs in the axisymmetric case and is eliminated when three-dimensional disturbances are considered.

The case $\epsilon_2/\epsilon_1 = -1\cdot0$, $\Omega_2 = \Omega_1 = 0$, $\delta = 0\cdot444$, and $\gamma = 5\cdot0$ was studied in greater detail. For $n = 1$ we found $a_c = 4\cdot1$ and $\tilde{R} = 97\cdot201$. For $n = 2$, a_c dropped to $3\cdot0$ and $\tilde{R}$ to $86\cdot985$. This seems to indicate a trend toward a purely azimuthal mode. Modulation of the outer cylinder only ($\epsilon_2 \neq 0$, $\epsilon_1 = \Omega_1 = \Omega_2 = 0$) was also studied in greater detail for higher values of n. For the case with $\gamma = 2\cdot0$, we found that for $n = 3$, $a_c \to 0$ with $\tilde{R} = 55\cdot764$; however, we had to use a Galerkin order $M = 6$ to obtain this result. When evaluating the stability limit for higher values of n, an even higher approximation order M was required. This hindered the search for n_c, since the evaluation of coefficients for matrix **D** in (22) becomes very expensive. A similar phenomenon was observed in the steady case shown in figure 10. We found that for increasingly negative values of Ω_2/Ω_1, n_c increases, and as our stability-limit search proceeds for higher values of n, the value of M required for convergence increases simultaneously. These results strongly point toward the possibility of inducing instability by a predominately outer-cylinder rotation through a purely azimuthal mode in both the steady and unsteady cases. This assertion can only be proved, however, after making our numerical scheme more efficient in order to reduce the prohibitive cost of computer time now required.

5. Conclusions

The small-gap approximation, which would have reduced this problem to a simpler Cartesian geometry, was not used at any time in this work. In this approximation one neglects all terms containing r (or β in non-dimensional units) in the denominator, since they are assumed to be of order δ (the non-dimensional gap size). The small-gap approximation used quite extensively by other investigators has been found to render rather good results for the steady Taylor-flow configuration. When considering unsteady flows, however, one must show that a term is indeed small for all time before it can be neglected. A striking example where the small-gap approximation is not valid for our problem is demonstrated in figure 4 where we show that the term V/β cannot be disregarded. By retaining these terms in the formulation, thus not restricting ourselves to cases where δ is small, we can extend the scope of our investigation to gaps of finite length with their many envisioned physical applications.

The first results presented were the linear stability bounds for both zero-mean and non-zero-mean flows, subject to axisymmetric disturbances ($n = 0$, $k \neq 0$). We compare our results with those of Thompson (1968) and Riley & Laurence (1976) for modulation of the inner cylinder about a zero mean (see figure 3). Thompson performed extensive laboratory experiments and in addition calculated a few points theoretically using finite differences. Our results are in good agreement with his. Unlike Thompson, Riley & Laurence used the small-gap approximation and reported some rather peculiar behaviour. For the stability limit $\tilde{R}$ they reported a derivative discontinuity along with a jump discontinuity for the critical wavenumber a_c at $\gamma = 1\cdot5$. In addition, their stability boundary was higher than ours or Thompson's. For non-zero-mean modulation of the inner cylinder, we found that at low frequencies, $\tilde{R}$ approaches $\tilde{R}_0\Omega_1/(\Omega_1 + \epsilon_1)$ while as $\gamma \to \infty$, it asymptotically approaches the limit for the steady mean flow $\tilde{R}_0$. Stabilization was not found at any frequency or modulation amplitude and $\tilde{R}$ was shown to be independent of the amplitude ratio ϵ_1/Ω_1. This again contrasts the findings of Riley & Laurence and can again be attributed to their usage of the

narrow-gap approach (see the appendix). Sinusoidal motion of the outer cylinder was also considered and we found that $\tilde{R}$ approaches ∞ for $\gamma \to 0$ or $\gamma \to \infty$, while it reaches a minimum near $\gamma = 2 \cdot 0$. Here the fluid seems to be at resonance, which is, however, damped by viscosity. This result contradicts the one obtained for steady rotation of the outer cylinder, which is always stable. Modulation of both cylinders in phase and out of phase was shown to have similar behaviour with $\epsilon_1 = \epsilon_2$ being the most destabilizing. Half-frequency response was found only for small γ and when motion of the outer cylinder was involved.

For non-zero-mean modulation, stabilization was found to be possible only for cases with $\epsilon_2 \neq 0$. In summary, for the axisymmetric case, we can conclude that the effect of modulation is most noticeable for small γ and then decreases in importance as $\gamma \to \infty$.

In the general three-dimensional non-axisymmetric case ($n \neq 0$, $k \neq 0$) for modulation of the inner cylinder only, we determined that axisymmetric disturbances ($n = 0$, $k \neq 0$) are the critical ones. This is consistent with the experimental data obtained by Thompson. When the outer cylinder is modulated (with or without the inner cylinder) we found that as γ increases, non-axisymmetric disturbances become the critical ones. This gives us an insight into the mechanism of instability. For steady or sinusoidal motion of the inner cylinder ($\epsilon_2 = \Omega_2 = 0$), the instability is dominated by centrifugal effects of the type mentioned by Rayleigh (1920) for the inviscid case (an adverse distribution of angular momentum). Modulation of the outer cylinder at low frequencies exhibits the same type of adverse angular-momentum distribution as for inner-cylinder motion. As γ increases, however, the shear effects become important and the secondary flow acquires a wave component in the azimuthal direction. Whether any purely azimuthal modes ($n \neq 0$, $k = 0$) exist or whether there is a sudden transition to turbulence are still open questions. In the non-zero-mean case

$$(\epsilon_1/\Omega_1 = -\epsilon_2/\Omega_1 = 0 \cdot 5 \quad \text{and} \quad \Omega_2 = 0)$$

we can conclude that the possible stabilization at higher frequencies found in the axisymmetric case will not occur in the three-dimensional non-axisymmetric case.

Appendix

In table 5 we present some numerical checks on our stability limit search for the unsteady Taylor flow. We chose to discuss the zero-mean modulation of the inner cylinder as an example. The first entries in table 5 show the stability limit $\tilde{R}$ and critical wavenumber a_c calculated for $\gamma = 1 \cdot 4$ and with Galerkin order M varying from 2 to 6. From this we see that our solution has essentially converged upto three significant figures for $M = 3$. In this paper we assumed convergence as a guideline, when the Taylor number $\tilde{R}$ for M was within 2 % of the one obtained for $M + 1$. The next few entries are stability limits calculated for $\gamma = 1 \cdot 6$. These calculations were made with $M = 2$, 4 and 6 for the purpose of finding out whether or not any discontinuities in the critical wavenumber a_c exist, as reported by Riley & Laurence in their earlier study. We found no such discontinuity for the small gap $\delta = 0 \cdot 0444$.

γ	M	a_c	$\tilde{R}$	δ
1·4	2	3·106	47·883 617 9	0·0444
1·4	3	3·123	47·605 728 4	0·0444
1·4	4	3·123	47·602 232 7	0·0444
1·4	5	3·124	47·587 689 9	0·0444
1·4	6	3·124	47·587 560 2	0·0444
1·6	2	3·114	48·552 378 7	0·0444
1·6	4	3·132	48·263 956 1	0·0444
1·6	6	3·134	48·248 552 8	0·0444
1·5	4	3·127	47·864 194 6	0·0444
1·5	4	3·126	46·929 420 5	0·0100
1·5	4	3·126	46·686 659 1	0·0010
1·5	4	3·126	46·662 416 6	0·0001
1·4	4	3·122	46·394 361 5	0·0001
1·6	4	3·131	47·068 315 6	0·0001

TABLE 5. Numerical checks of the stability search algorithm.

Next we evaluated a_c and $\tilde{R}$ for $\gamma = 1\cdot5$, $M = 4$ for a decreasing sequence of small gaps $\delta = 0\cdot0444$, $0\cdot0100$, $0\cdot0010$ and $0\cdot0001$. These results show no evidence of a qualitative change in behaviour for a_c or $\tilde{R}$ as a function of γ as $\delta \to 0$. As a final check, we bracketed the point where Riley & Laurence reported a discontinuity ($\gamma = 1\cdot5$) and for a very small gap ($\delta = 0\cdot0001$) found a_c to be indeed a continuous function of γ. Other checks were also performed but for the sake of brevity will not be presented here. From these results, we concluded that Riley & Laurence's findings contrasted ours, mainly because they used an approximation which is not always justified for unsteady circular Couette flow.

REFERENCES

ABRAMOWITZ, M. & STEGUN, I. A. 1972 *Handbook of Mathematical Functions*. Dover.

CLEVER, R. M., BUSSE, F. H. & KELLY, R. E. 1977 Instabilities of longitudinal convection rolls in Couette flow. *Z. angew. Math. Phys.* **28**, 771–783.

COLES, D. 1965 Transition in circular Couette flow. *J. Fluid Mech.* **21**, 385–425.

DAVIS, S. H. 1976 The stability of time periodic flows. *Ann. Rev. Fluid Mech.* **8**, 57–79.

DONNELLY, R. F. 1964 Experiments on the stability of viscous flow between rotating cylinders. III. Enhancement of stability by modulation. *Proc. Roy. Soc.* A **781**, 130–139.

HALL, P. 1975 The stability of unsteady cylinder flows. *J. Fluid Mech.* **67**, 29–63.

HIDE, R. 1969 *The Global Circulation of the Atmosphere* (ed. G. A. Conley), pp. 196–221. Royal Meterological Soc.

KERCZEK, C. VON & DAVIS, S. H. 1974 Linear stability theory of oscillatory Stokes layers. *J. Fluid Mech.* **64**, 753–773.

KRUEGER, E. R., GROSS, A. & DIPRIMA, R. C. 1966 On the relative importance of Taylor vortex and non-axisymmetric modes in flow between rotating cylinders. *J. Fluid Mech.* **24**, 521–538.

OTHMER, H. G. 1976 Current problems on pattern formation. *Lectures on Mathematics in the Life Sciences* (ed. S. A. Levin). Providence, R.I.: The American Math. Soc.

PEDLOSKY, J. 1972 Limit cycles and unstable baroclinic waves. *J. Atmos. Sci.* **29**, 53–63.

RAYLEIGH, LORD 1920 On the dynamics of revolving fluids. *Scientific Papers*, vol. 6, pp. 447–453. Cambridge University Press.

RILEY, P. J. & LAURENCE, R. L. 1976 Linear stability of modulated circular Couette flow. *J. Fluid Mech.* **75**, 625–646.

SEMINARA, G. & HALL, P. 1976 Centrifugal instability of a Stokes layer: linear theory. *Proc. Roy. Soc.* A **350**, 299–316.

THOMPSON, R. 1968 Ph.D. thesis, Department of Meteorology, Massachusetts Institute of Technology.

TUSTANIWSKYJ, J. I. 1979 Ph.D. thesis, Department of Mechanical Engineering, Wayne State University.

YIH, C. S. & LI, C. H. 1972 Instability of unsteady flows or configuration. Part 2. Convective instability. *J. Fluid Mech.* **54**, 143–152.